

Analysis of observational data from Extreme Ultra-Violet Camera onboard Chang'E-3 mission

Yan Yan^{1,2,3} · Hua-Ning Wang^{1,2} · Han He^{1,2} · Fei He⁴ · Bo Chen⁴ · Jian-Qing Feng¹ · Jin-Song Ping¹ · Chao Shen⁵ · Rong-Lan Xu⁶ · Xiao-Xin Zhang⁷

Received: 23 October 2015 / Accepted: 2 January 2016 / Published online: 22 January 2016
© Springer Science+Business Media Dordrecht 2016

Abstract The Extreme Ultra-Violet Camera (hereafter EUVC) is a scientific payload onboard the lander of the Chang'E-3 (hereafter CE-3) mission launched on December 1st, 2013. Centering on a spectral band around 30.4 nm, EUVC provides the global images of the Earth's plasmasphere from the meridian view, with a spatial resolution of $0.1 R_{\oplus}$ in 150×150 pixels and a cadence of 10 minutes. Along with the data being publicly released online, some unsettled issues in the early stage have been clarified, including the geometrical preparations, the refined approach on the coefficient K for the background, and the alignment among the images. A demo of data after all the above processes is therefore presented as a guidance for users who are studying the structure and dynamics of the plasmasphere.

Keywords Earth: plasmasphere · Space vehicles: instruments · CE-3 Extreme Ultra-Violet Camera · Techniques: image processing

✉ Y. Yan
yyan@bao.ac.cn

- 1 National Astronomical Observatories, Chinese Academy of Sciences, Beijing 100012, China
- 2 Key Laboratory of Solar Activity, Chinese Academy of Sciences, Beijing 100012, China
- 3 University of Chinese Academy of Sciences, Beijing 100049, China
- 4 Changchun Institute of Optics, Fine Mechanics and Physics, Chinese Academy of Sciences, Changchun 130033, China
- 5 School of Natural Sciences and Humanity, Harbin Institute of Technology Shenzhen Graduate School, Shenzhen 518055, China
- 6 State Key Laboratory of Space Weather, National Space Science Center, Chinese Academy of Sciences, Beijing 100190, China
- 7 National Center for Space Weather, China Meteorological Administration, Beijing 100081, China

1 Introduction

CE-3, as part of the second phase of China's Lunar Exploration Program (hereafter CLEP), has been softly landing onto the Moon, with lots of scientific payloads, in order to implement experiments as a selenomorphological measurement, astronomical observation, and plasmaspheric imaging. The general perspective on CE-3 and payloads within is surveyed (Ip et al. 2014). Among the scientific payloads, EUVC mounted on the CE-3's lander is an Extreme Ultra-Violet Camera, studying the structure and dynamics of the Earth's plasmasphere by means of imaging it at the spectral band of 30.4 nm from the meridian perspective (Chen et al. 2014, hereafter C14).

The Earth's plasmasphere, sandwiched between the ionosphere and magnetosphere, generally regarded as a reservoir filled with cold and dense plasmas from the former along geomagnetic field lines, was first identified by whistlers observations in the late 1940s (Storey 1953; Carpenter 1963). After some decades, fruitful results both on theoretical modeling and observational characteristics were seen. In the meantime, some new observational techniques have been progressing, boosting our understanding of the plasmasphere into a higher horizon in many respects. The most highlight one among them should be the Imager for Magnetopause-to-Aurora Global Exploration (hereafter IMAGE) (Burch et al. 2001), which carried two powerful instruments. One, the radio plasma instrument (RPI), is mainly responsible for measuring the electron density by means of radio wave sounding, while the other, the extreme ultraviolet (EUV) imager (Sandel et al. 2000, 2003) takes photographs of the plasmasphere from the aerial view (also referring to the face view) through a 30.4-nm filter. The reason why the spectral line is chosen is definitely that He^+ ions, constituting some one-fifth of the plasmaspheric substance, can

resonantly scatter the 30.4-nm sunlight, enabling us to visualize it. A comprehensive but precise review including the observation results prior to 2008 was written (see Darrouzet et al. 2008 and references within). Another following-up imager is the Telescope of EXtreme ultraviolet (TEX) aboard Japan's lunar orbiter (KAGUYA) (Yoshikawa et al. 2008), from the meridian view. It is to be regretted that no global images from the meridian view are obtained, as a result of the vibration or shock inducing mechanical damage of the metal band-pass filter at its launch (Yoshikawa et al. 2010). EUVC, the optical design alike, is a lunar-based and fixed camera globally imaging the plasmasphere at 30.4 nm from the meridian view (side view), investigating the observational characteristics and reflections corresponding with the one facing on. Still, any novel structures will be expected. The detailed ground calibration of EUVC was addressed by C14. Prior to CE-3 mission's launch, He et al. (2011) had made a careful plasmaspheric reconstruction from the moon-based observation by means of the Genetic Algorithm, and one had published a successive paper on a numerical simulation (He et al. 2013).

This paper is arranged into a few independent parts. Section 2 details the instrumental parameters and data products. Section 3 is a geometry-focused part, introducing some geometric preparations and their related procedures. Section 4 pays special attention to data processing, including de-noising and alignment. An initial demo is shown in Sect. 5. Section 6 will address the emission intensity and column density of He II of the plasmasphere in the side view. Finally, a summary and a discussion will be given in Sect. 7.

2 Instrumentation and data products

The section is a brief introduction of the instrumentation and data products.

2.1 Instrumentation

For pursuing both a smaller volume and a wider field of view (hereafter FoV), a single spherical mirror and a spherical detector, a microchannel plate (MCP), is applied to EUVC's optical design (Chen and He 2011; C14). The instrument, with a thin filter in front of the mirror to filter out the sunlight other than 30.4 nm, is an imager fabricated on CE-3's lander, with a FoV of 14.7° and an angular resolution of 0.08° based on their calibration tests. The test results of EUVC, considered as technical parameters, are listed in Table 1, adapted from C14. Before launch, they also performed geometric and radiometric calibration at the Changchun Institute of Optics, Fine Mechanics and Physics, Chinese Academy of Sciences.

Table 1 Test results of EUVC

Parameter	Value
Center wavelength (nm)	30.2
Bandwidth (nm)	4.6
Sensitivity ratio at 30.4 nm and 58.4 nm	79.2
FoV (°)	14.7
Angular resolution (°)	0.08
Exposure time (min)	10
Dynamical range (Rayleigh)	0.1–10
Sensitivity (count s ⁻¹ Rayleigh ⁻¹)	0.11

Note: Adapted from C14

CE-3 was launched from the Xichang Satellite Launch Center, located at Sichuan Province, Southwest of China, on December 1st, 2013. After a long journey with multi-orbit-changing, it correctly performed a soft landing at 19.51°W, 44.12°N of the Moon on December 14th, 2013 (Ip et al. 2014) successfully. By means of a short adjustment, EUVC became operational soon afterwards. A symbol referring to the data will be highlighted on China's official media—the Xinhua Net, as soon as possible.

The paper on preliminary data processing was investigated (Feng et al. 2014, hereafter F14), however, it required a deeper analysis and further revision to follow. For ease of performing scientific research, other essential tasks for data processing should be performed. Two of them will be carefully treated in Sects. 3 and 4.

2.2 Data products

The data are retrieved and distributed from the Science and Application Center for Moon and Deep Space Exploration, affiliated with National Astronomical Observatories, Chinese Academy of Sciences (NAOC) (F14). A collective of datasets, produced by the Ground Research and Application System of CLEP, is available online now. The website from which one can download the datasets is <http://moon.bao.ac.cn/ceweb/datasrv/dmsce3.jsp>. It requires a short registration first. The data policy is that the datasets are freely distributed and used by worldwide users. The camera needs to keep away from the direct sunlight; hence, it is cut off at all the lunar noons. The best observation schedule should therefore be arranged in lunar mornings and dusks. In fact, there had been six working windows as follows, almost each one in a month, 388 in total from December 24, 2013 to May 20, 2014 on six lunar-days; refer to Table 2 for details. The formatted database only includes two types of Level-2 products, Level-2A and Level-2B, whereas Level-2B data products are used to do scientific research.

Fig. 1 The filename of an EUVC Level-2B product on December 24th, 2013

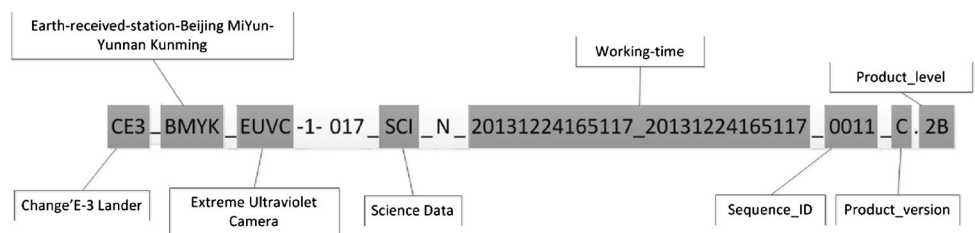


Table 2 Data products of each working window

Number	Universal time (YYYY/MM/DD/HH/MM/SS)	Data sample
1	20131224165117–20131224170138	2
2	20140122191247–20140122203540	9
3	20140221002623–20140221233003	119
4	20140322115933–20140322235847	65
5	20140420210249–20140422011007	153
6	20140520110307–20140520184204	40
Total	20131224165117–20140520184204	388

The format of the scientific data is of the Planetary Data System (hereafter PDS), originally created by the National Aeronautics and Space Administration (NASA), using to lay up solar-terrestrial data. The illustration of the filename is depicted in Fig. 1 in detail.

3 Geometric positioning of the images

A first look of the plasmasphere is readily taken, and the morphology appears dipole-like. However, the coming qualitative analysis needs a precise position-fixing first. This section will give some essential geometric preparations before the data can be evaluated.

3.1 Camera coordinate system and coordinate transformation

The geometric parameters written in the head label of each data are in terms of the solar-magnetic coordinate system (hereafter SMS), and in units of the SI. SMS, generally adopted by the space science community, serves for any global structures which are symmetrical with regard to the magnetic equatorial plane, e.g. the plasmasphere. In contrast, if we want to do some calculations, the most helpful information should be evaluated in the camera coordinate system (hereafter CMS). The X_{CMS} axis refers to the vector of the optical axis pointing from the Earth to the FOV of EUVC, while the YZ plane, perpendicular to the X_{CMS} axis, is the projection plane of the images. On the plane, the

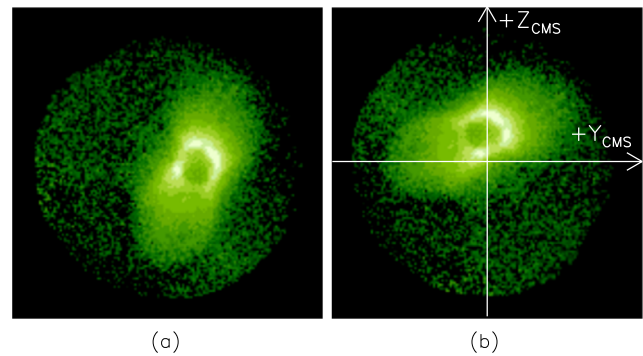


Fig. 2 The reversal of an EUVC Level-2B product observed at UTC 201312241651. (a) and (b) are both shown logarithmically. The morphology of (b) is adopted hereafter

Z_{CMS} axis means the local north of the moon, and the Y_{CMS} is determined by the right-hand law. The two axes of the YZ plane are illustrated in Fig. 2(b).

The coordinate transformation for the two coordinate systems can be written

$$\mathbf{V}_{CMS} = \mathbf{T} \cdot \mathbf{V}_{SMS}, \quad \text{or} \quad \mathbf{V}_{SMS} = \mathbf{V}_{CMS} \cdot \mathbf{T}, \quad (1)$$

where \mathbf{V}_{CMS} or \mathbf{V}_{SMS} is the position vector in each Cartesian coordinate system, and \mathbf{T} represents the transformation tensor, an element of which is the cosine of the angle between each component of the two unit vectors.

Based on the way of data reading of EUVC, we shall make an adjustment to the morphology. Figure 2(a) presents the uncorrected online data, whereas it is intended to be adjusted into Fig. 2(b), in accordance with the defined CMS. The transformation can be fulfilled under mutually exchanging rows and columns of the matrix.

3.2 Determination of the projection of the geocenter

Another geometric benchmark that should be pre-considered is the exact position of the projection of the geocenter on each image. The algorithm is written thus:

$$\mathbf{V}_{\oplus} = (V_1, V_2, V_3), \quad (2)$$

$$\theta = 90 - \arcsin V_1, \quad (3)$$

$$\phi = \arctan \frac{V_3}{V_2}, \quad (4)$$

$$dx = \theta \cdot \cos \phi / \delta, \quad (5)$$

$$dy = \theta \cdot \sin \phi / \delta, \quad (6)$$

where \mathbf{V}_{\oplus} indicates the unit vector of geocenter-pointing in CMS, θ and ϕ are the deflections of polar angle and azimuthal angle in degrees, δ means the angular resolution, and dx and dy are the deviations to the center of the image in pixels.

4 Data processing

The data processing of the images from EUVC contains two sub-sections. The first one is mostly concerned with de-noising for eliminating the background, whereas the second one works for the alignment of the images on each working window.

4.1 De-noise for eliminating the background

The de-noising for eliminating the background is a matter of prime importance. Various factors may induce multifarious noises, e.g. the energetic electrons (Yan et al. 2016). Among them, the noise coming from the scatter light of the sky background plays a vital role on the lowering down of the signal-to-noise ratio of the images. On account of this, an efficient and reliable method must be carried out first.

In the earlier work, as Sect. 4 of F14 treated of, there was an eight-step data processing. Later on, the Scientific Team (hereafter ST) thought that it still needed some refinement. After reaching the consensus in a workshop, ST decided to merely revise the last step of the data processing, while reserving the other steps. In their paper, the eighth step is just to seek out a factor K to perform the optimal background removal with a belt region, sandwiched between 55 and 66 pixels away from the center of the image. However, we consider it as less-refined to give a homogeneous value to the 2D data, with a distribution in different parts. An improved algorithm is thus established to give a K distribution by means of cutting the belt region into six equal fan-shaped parts with 60° central angle each; see Fig. 3. The final version K is a matrix after smoothness and interpolation. Except for the manipulation, we agree on the magnification of K with 1.1 times the original value in the end. The angular distribution of the K matrix is illustrated in Fig. 4.

4.2 Alignment among the images

Except for de-noising, the alignment is another indispensable job one should pre-consider. Without perfect alignment, the arrangement is quite inconvenient in the following-up study, in particular, e.g. the temporal-evolution analysis. The

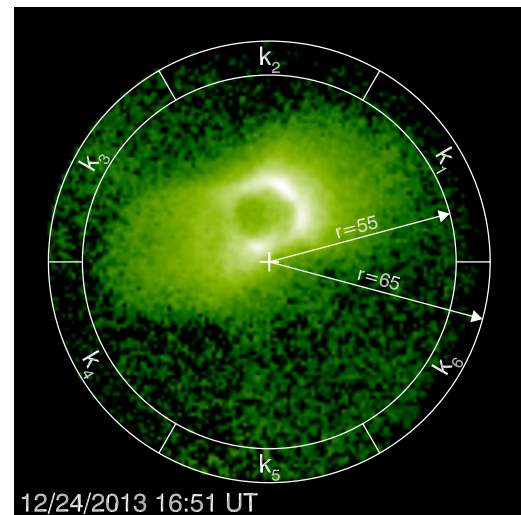


Fig. 3 Sketch of different K in six equal fan-shaped parts

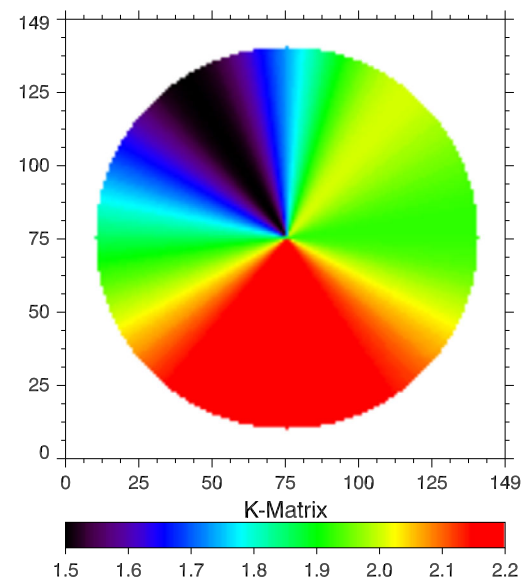


Fig. 4 Angular distribution map of K -matrix. The anisotropy is clear, while the bottom part is larger than the counterpart in this case

images from EUVC are available covering six-month observations. In Sect. 3.2, although there has been an algorithm to calculate the projection of the geocenter on the image, we find that there are still shifts on the consecutive images of each observational window. Worse still, there is no obvious rule. It would be a troublesome problem for quantitative analysis. The only thing we can do is to look for an approach to achieve the alignment of the images. The cross-correlation methodology in Digital-Image-Processing is used frequently in medical care, remote sensing, military-target tracking, and natural-science related fields. Recently, cross-correlation has made great progress, leading to a multitude of distinguished aligning methods. We decided to employ cross-correlation in a simulated template with brief-

Fig. 5 Diagrams illustrating the method of the alignment of the images. Panel (a) shows the cutting horizontal slice, and (b) plots the distribution of the slice. Panel (c) presents the simulated template for cross-correlation, while (d) plots the distribution of the template

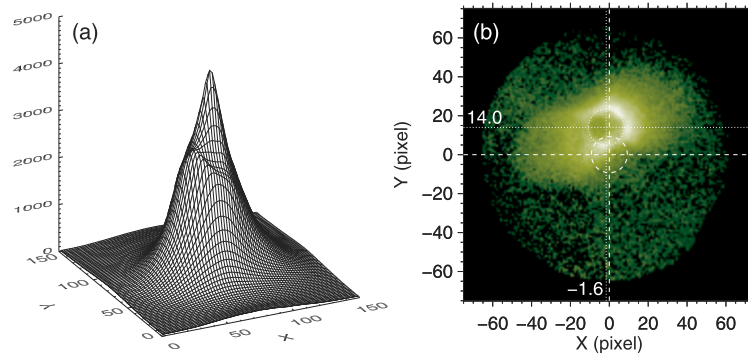
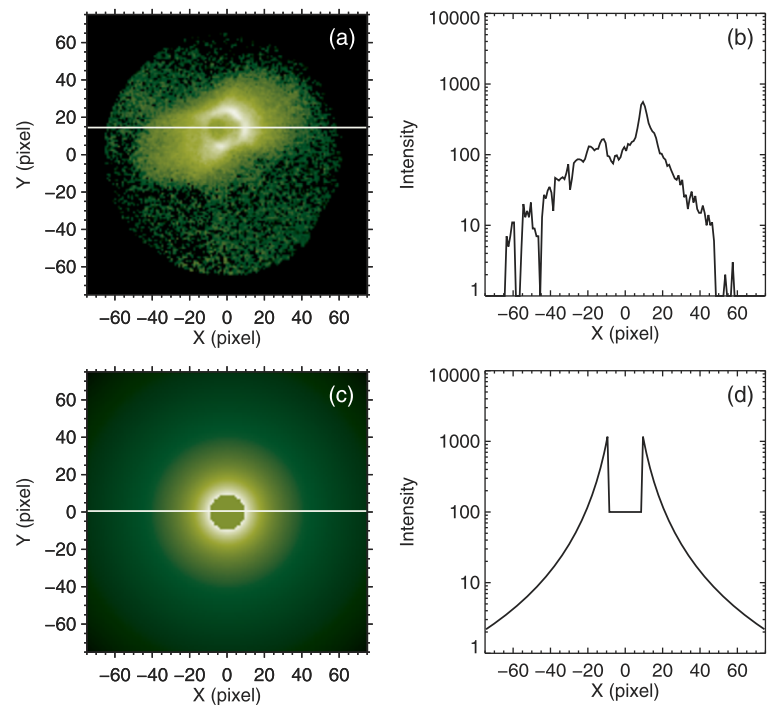


Fig. 6 Results of the determination of the geocenter with the cross-correlation method applied to the data and template. Panel (a) depicts the output of the cross-correlation, while (b) points out the position of the geocenter. The *cross dashed lines* plotted on (b) are the *middle lines* of the image, while the *cross dotted lines* act as the deviation to the *middle lines*. The intersection of the *dotted lines* is considered to be the geocenter.

ness and practicality, because the consecutive images do not appear rather complicated or to have over-distorted structures.

On this issue, early work was reported in Zheng et al. (2015). Analogously, we will give a concise, but still solid method on the alignment of the images. First of all, we cut a horizontal slice (Fig. 5(a)) to make a statistical distribution analysis for creating a template (see Fig. 5(b)). Owing to the distribution, a simulated template will be produced (see Fig. 5(c)) and prepared for later use on the cross-correlation, the distribution of the template plotted in Fig. 5(d). Afterward, we apply the cross-correlation method to seek out the best position with the maximum correlation coefficient, which belongs to the geocenter (see Figs. 6(a) and (b)).

5 Demo

After the above processes, EUVC data are well prepared and can be implemented in scientific research. Subsequently, 388 data samples picked up in six observation windows (with various geomagnetic conditions) have been officially released. For using the data more handily and practically, we have developed another type of product. The product has been adjusted with the geocenter to the center of the image and with rotation of the north magnetic axis to the upward of the image by means of a cubic convolution interpolation (Park and Schowengerdt 1983). The objective of the operation is to study the physical evolution of the plasmasphere, eliminating to the utmost any influence of revolving on its

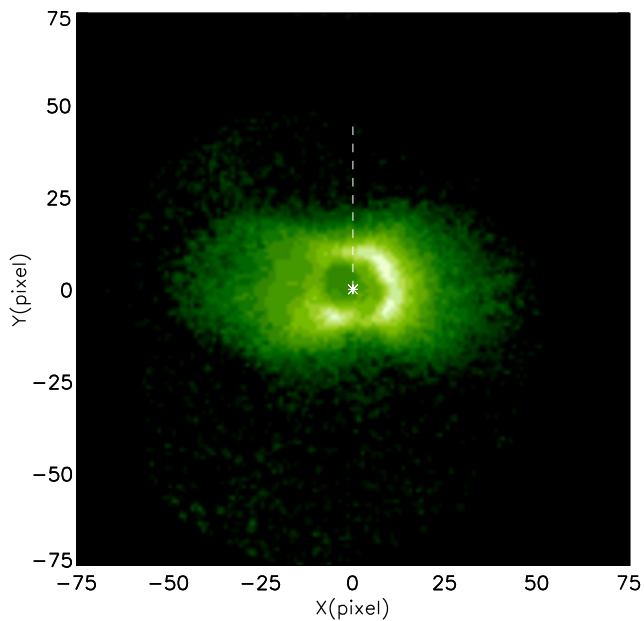


Fig. 7 New type data with the filename 20131224165117. The *dash line* acts as the north magnetic axis, penetrating the north magnetic pole from the geocenter, also as the upward of the image

own axis. Figure 7 shows the preceding example in the type, restraining the background-noise moderately.

6 Emission intensity and column density of He II of plasmasphere

6.1 Emission intensity

It is feasible to convert the count into the emission intensity through Eq. (7) (C14),

$$I = \frac{N}{t \cdot S}, \quad (7)$$

where I means the emission intensity in Rayleigh, N represents the count in each pixel, t is the exposure time, and S acts as the sensitivity.

6.2 Column density

The He II solar emission (30.4 nm) is a landmark emission line to study solar chromospheric activity and also an essential factor to ionize and heat the Earth's upper atmosphere (Worden et al. 1999). Fortunately, He⁺ ions, the second abundant constituent of the plasmasphere (Craven et al. 1997) can scatter the solar irradiance through a resonantly scatter process. The scattered 30.4-nm emission from the plasmasphere is optically thin; therefore, the measured brightness is directly proportionally to the He II column density along the line of sight through the plasmasphere (Meier

1991). IMAGE has given the global He II column density from the top view, convincing us of the feasibility of applying the same method to imaging the plasmasphere from the side view.

We can calculate the column density of He II from (Garido et al. 1994)

$$4\pi I = \int e^{-\tau} p(\theta) gn(\mathbf{r}) ds \times 10^{-6}, \quad (8)$$

where I is the emission intensity calculated by Eq. (7), τ is the optical depth, mostly regarded as zero due to the optical thinness, g is the scattering rate, which is proportional to the solar 30.4-nm flux, n is the number density at position \mathbf{r} , and $p(\theta)$ represents the scattering phase function, given by $p(\theta) = 1 + 1/4(2/3 - \sin^2 \theta)$, where θ is the angle between the sun-earth direction and the vision direction. The column density can therefore be evaluated. In addition, the solar 30.4-nm flux was available online with ultra-high time-resolution (Didkovsky et al. 2012), and the data are easily examined. While g has a linear relationship with the solar 30.4-nm flux, one may catch the rapid brightening induced by solar flares, because the other parameters are slowly and continuously varied.

7 Summary and discussion

The EUVC onboard CE-3 mission is devoted to providing the first global images of the Earth's plasmasphere from the meridian view. Level-2B data products, serving as scientific research, have been available to the scientific community. After the efficient and reliable de-noising, in the images has appeared roughly the dipole-like morphology which would be expected by previous models. The qualitative or morphological studies can therefore be evaluated. The determination of the plasmapause based upon the EUVC data has been carried out (He et al. 2016), and the result agrees with the observations from other satellites. In addition, more accurate geometric positioning determined in sub-pixel resolution also makes doing a quantitative analysis feasible, e.g. time-series analysis. It would be beneficial to study the dynamics of the inner magnetosphere under various geophysical conditions (Darrouzet and De Keyser 2013). The global meridian images could be good Lydian-stones checking the earlier models and making a comparison with their corresponding simulation or reconstruction results.

Beyond this, we have developed another type of product, in Sect. 6, easily and flexibly used to study the dynamics of the plasmasphere. If someone who is interested in them, please contact us in personal communication, or we could release the dataset unofficially in the near future.

The first global column density of He II of the plasmasphere from the meridian view can be calculated from the

images taken by EUVC. Thanks to the high time-resolution data of solar 30.4-nm flux, we may study the column density of the plasmasphere responding to the surge of the flux of solar 30.4-nm radiation, e.g. solar flares. Still, it is feasible to do a sophisticated study of the variation for months due to the inter-monthly variation of solar 30.4-nm flux.

It is for the first time that one has a consecutive panorama of the Earth's plasmasphere from the meridian view in considerable temporal and spatial resolution. Accordingly, any novel structures in all kinds of scales seen from the side view would be well observed and followed on time. Still further, the more interesting thing is that we might encounter the counterparts of the structures recorded by IMAGE from the top view.

Acknowledgements The contributions from the EUVC design and calibration team at the Changchun Institute of Optics, Fine Mechanics and Physics, Chinese Academy of Sciences, and the data processing team at the Science and Application Center for Moon and Deep Space Exploration, affiliated with the National Astronomical Observatories of China are both well appreciated. This work is primarily supported by the Key Research Program of the Chinese Academy of Sciences through grant Y422013V01-CE-3.

References

- Burch, J.L., Mende, S.B., Mitchell, D.G., et al.: Views of Earth's magnetosphere with the IMAGE satellite. *Science* **291**, 619 (2001)
- Carpenter, D.L.: Whistler evidence of a "knee" in the magnetospheric ionization density profile. *J. Geophys. Res.* **68**(6), 1675 (1963)
- Chen, B., He, F.: Optical design of moon-based Earth's plasmaspheric extreme ultraviolet imager. *Opt. Precis. Eng.* **19**, 2057 (2011) (in Chinese)
- Chen, B., Song, K.-F., Li, Z.-H., et al.: Development and calibration of the Moon-based EUV camera for Chang'e-3. *Res. Astron. Astrophys.* **14**, 1454 (2014)
- Craven, P.D., Gallagher, D.L., Comfort, R.H.: Relative concentration of He⁺ in the inner magnetosphere as observed by the DE 1 retarding ion mass spectrometer. *J. Geophys. Res.* **102**(A2), 2279 (1997)
- Darroutet, F., De Keyser, J.: The dynamics of the plasmasphere: recent results. *J. Atmos. Sol.-Terr. Phys.* **99**, 53 (2013)
- Darroutet, F., Gallagher, D.L., André, N., et al.: Plasmaspheric density structures and dynamics: properties observed by the CLUSTER and IMAGE missions. *Space Sci. Rev.* **145**, 55 (2008)
- Didkovsky, L., Judge, D., Wieman, S., Woods, T., Jones, A.: EUV SpectroPhotometer (ESP) in extreme ultraviolet variability experiment (EVE): algorithms and calibrations. *Sol. Phys.* **275**, 179 (2012)
- Feng, J.-Q., Liu, J.-J., He, F., et al.: Data processing and initial results from the CE-3 Extreme Ultraviolet Camera. *Res. Astron. Astrophys.* **14**, 1664 (2014)
- Garrido, D.E., Smith, R.W., Swift, D.W., et al.: Imaging the plasmasphere and trough regions in the extreme-ultraviolet region. *Opt. Eng.* **33**, 371 (1994)
- He, F., Zhang, X.-X., Chen, B., Fok, M.-C.: Reconstruction of the plasmasphere from moon-based EUV images. *J. Geophys. Res.* **116**, A11203 (2011)
- He, F., Zhang, X.-X., Chen, B., Fok, M.-C., Zou, Y.-L.: Moon-based EUV imaging of the Earth's plasmasphere: model simulations. *J. Geophys. Res.* **118**, 7085 (2013)
- He, F., Zhang, X.-X., Chen, B., Fok, M.-C.: Determination of the Earth's plasmapause location from the CE-3 EUVC images. *J. Geophys. Res.* (2016). doi:[10.1002/2015JA021863](https://doi.org/10.1002/2015JA021863)
- Ip, W.-H., Yan, J., Li, C.-L., Ouyang, Z.-Y.: Preface: the Chang'e-3 lander and rover mission to the Moon. *Res. Astron. Astrophys.* **14**, 1511 (2014)
- Meier, R.R.: Ultraviolet spectroscopy and remote sensing of the upper atmosphere. *Space Sci. Rev.* **58**, 185 (1991)
- Park, S., Schowengerdt, R.: Image reconstruction by parametric cubic convolution. *Comput. Vis. Graph. Image Process.* **23**, 256 (1983)
- Sandel, B.R., Broadfoot, A.L., Curtis, C.C., et al.: The extreme ultraviolet imager investigation for the IMAGE mission. *Space Sci. Rev.* **91**(1/2), 197 (2000)
- Sandel, B.R., Goldstein, J., Gallagher, D.L., Spasojevic, M.: Extreme ultraviolet imager observations of the structure and dynamics of the plasmasphere. *Space Sci. Rev.* **109**, 205 (2003)
- Storey, L.R.O.: An investigation of whistling atmospherics. *Philos. Trans. R. Soc. Lond.* **246A**, 113 (1953)
- Worden, J., Woods, T.N., Neupert, W.M., Delaboudinière, J.: Evolution of chromospheric structures: how chromospheric structures contribute to the solar He II 30.4 nanometer irradiance and variability. *Astrophys. J.* **511**, 965 (1999)
- Yan, Y., Wang, H.-N., Shen, C., Du, Z.-L.: A substorm-associated enhancement in the XUV radiation measuring channel observed by ESP/EVE/SDO. *Res. Astron. Astrophys.* (2016, in press)
- Yoshikawa, I., Yamazaki, A., Murakami, G., et al.: Telescope of extreme ultraviolet (TEX) onboard SELENE: Science from the Moon. *Earth Planets Space* **60**, 407 (2008)
- Yoshikawa, I., Murakami, G., Ogawa, G., et al.: Plasmaspheric EUV images seen from lunar orbit: initial results of the extreme ultraviolet telescope on board the Kaguya spacecraft. *J. Geophys. Res.* **115**, A04217 (2010)
- Zheng, C., Ping, J.-S., Wang, M.-Y., Li, W.-X.: Geocentric position preliminary detection from the Extreme Ultraviolet Images of Chang'e-3. *Astrophys. Space Sci.* **358**, 28 (2015)